WIRELESS COMMUNICATIONS AND MOBILE COMPUTING
Wirel. Commun. Mob. Comput. 2009; **9**:705–717
Published online 7 April 2008 in Wiley InterScience
(www.interscience.wiley.com) DOI: 10.1002/wcm.623

Ranging error-tolerable localization in wireless sensor networks with inaccurately positioned anchor nodes

Rongfei Fan[1], Hai Jiang[1*,†], Shaohua Wu[2] and Naitong Zhang[2]
[1]*Department of Electrical and Computer Engineering, University of Alberta, Canada*
[2]*School of Electronics and Information Technology, Harbin Institute of Technology, P.R. China*

Summary

Localization is essential for wireless sensor networks (WSNs). It is to determine the positions of sensor nodes based on incomplete mutual distance measurements. In this paper, to measure the accuracy of localization algorithms, a ranging error model for time of arrival (TOA) estimation is given, and the Cramer–Rao Bound (CRB) for the model is derived. Then an algorithm is proposed to deal with the case where (1) ranging error accumulation exists, and (2) some anchor nodes broadcast inaccurate/wrong location information. Specifically, we first present a ranging error-tolerable topology reconstruction method without knowledge of anchor node locations. Then we propose a method to detect anchor nodes whose location information is inaccurate/wrong. Simulations demonstrate the effectiveness of our algorithm. Copyright © 2008 John Wiley & Sons, Ltd.

KEY WORDS: wireless sensor networks; localization; Cramer–Rao Bound; topology reconstruction

1. Introduction

Localization is essential for wireless sensor networks (WSNs). It is to determine the positions of sensor nodes based on incomplete mutual distance measurements. Localization algorithms can be loosely categorized into two classes: ranging-based algorithms and ranging-free algorithms. Compared with ranging-free algorithms, ranging-based algorithms can achieve higher localization accuracy with fewer anchor nodes [1]. Traditional ranging methods are based on the time of arrival/time difference of arrival (TOA/TDOA), received signal strength (RSS), and angle of arrival (AOA). Among them, TOA is preferred because of its high ranging accuracy and relatively simple hardware structure, especially with the technique of ultra-wideband (UWB).

Specifically, localization is to estimate the positions of all the nodes in a network, given the positions of some nodes (referred to as *anchor nodes*) and partial pairwise distance measurements between neighboring nodes [2]. Two major challenges in localization are as follows. First, the accuracy of distance measurements may be degraded by noise (referred to as the *ranging error problem*). The impact of the ranging error usually depends on the estimation algorithm, the bandwidth of pulses, application scenarios, etc. [3,4]. It is difficult to take all the factors into account. Second, the position information provided by some anchor nodes may be inaccurate/wrong. For example, in a WSN for forest

*Correspondence to: Hai Jiang, Department of Electrical and Computer Engineering, University of Alberta, Canada.
†E-mail: hai.jiang@ece.ualberta.ca

fire detection, some anchor nodes may be moved by pedestrians or animals (thus referred to as *inaccurately positioned anchor nodes*). But the anchor nodes still broadcast their original positions, thus leading to localization errors.

In the literature, the ranging error problem has been investigated extensively. Using distance measurements and positions of anchor nodes, other nodes' relatively accurate positions can be calculated by Multilateration [5] or multidimensional scaling (MDS) [6] algorithm. Furthermore, to overcome the ranging errors, an optimization problem can be formulated to minimize some global error functions such as maximum likelihood estimation [7] and semidefinite programming [2,8]. Although these algorithms may guarantee estimation accuracy under certain conditions, most of them become vulnerable in the presence of inaccurately positioned anchor nodes.

In this paper, our objective is to solve both the ranging error problem and the inaccurate anchor node position problem simultaneously. We first analyze Cramer–Rao Bound (CRB) for localization in a WSN. To measure the accuracy of a specific localization algorithm, CRB is studied in the literature [9,10], where ranging error between any pair of nodes is usually assumed to be independent and identically distributed. However, as shown in Subsection 2.2 of this paper, ranging error also depends on the distance between the two nodes. In this research, we present an ideal ranging error model in TOA estimation, and further derive the CRB for localization. Moreover, we propose a localization algorithm that consists of two steps: first, to estimate the network topology (i.e., relative positions between nodes) without knowledge of anchor node locations, then to detect inaccurately positioned anchor nodes and further obtain the positions of all the nodes in the network. The rest of this paper is organized as follows. The CRB for localization is derived in Section 2. Sections 3 and 4 present the two steps in our localization algorithm, that is, topology reconstruction and detection of inaccurately positioned anchor nodes, respectively. The performance evaluation is given in Section 5, followed by concluding remarks in Section 6.

2. CRB for Localization

2.1. Network Model

Assume that all the nodes in a WSN are fixed on a plane. There are M sensors (with IDs from 1 to M) without position information and $N - M$ sensors (with IDs from $M + 1$ to N) with known position information, referred to as *non-anchor nodes* and *anchor nodes*, respectively. Non-anchor nodes form a set $\mathcal{Q}$, while anchor nodes form a set $\mathcal{P}$. Node i can communicate with node j and thus can measure the distance to node j if and only if the distance between nodes i and j, that is, $d_{i,j}$, is less than the *visible radius R*. All the nodes that can communicate with node i form a set denoted as $\mathcal{F}(i)$. Define a distance measurement set $\mathcal{D}$ in which

$$\mathcal{D} = \left\{\hat{d}_{i,j} | i \in \mathcal{P} \cup \mathcal{Q},\ j \in \mathcal{F}(i)\right\} \tag{1}$$

where $\hat{d}_{i,j}$ is the measured distance between nodes i and j. Our objective is to use set $\mathcal{D}$ and position information of anchor nodes, $\mathcal{W}_{\mathcal{P}}$, where

$$\mathcal{W}_{\mathcal{P}} = \left\{(x_i, y_i)^{\mathrm{T}} | i \in \mathcal{P}\right\} \tag{2}$$

to reconstruct the set

$$\mathcal{W}_{\mathcal{Q}} = \left\{(x_i, y_i)^{\mathrm{T}} | i \in \mathcal{Q}\right\} \tag{3}$$

where the superscript T means transpose, $(x_i, y_i)^{\mathrm{T}}$ is coordinate vector of node i, and $\mathcal{W}_{\mathcal{P}}$ and $\mathcal{W}_{\mathcal{Q}}$ denote the set of coordinate vectors of anchor nodes and non-anchor nodes, respectively. Throughout the paper, if z means the coordinate of a node or the distance between two nodes, we use $\hat{z}$ to denote the measured or estimated value of z in the localization.

2.2. Ranging Error Model

As localization is based on ranging results among nodes, a well-built ranging error model can facilitate localization in the process of refinement. Ranging accuracy depends on a number of factors such as application scenarios, TOA estimation algorithms, and the bandwidth of pulses. Generally, it is difficult to construct a general ranging error model to take into account all the factors. So we use the lower bound of TOA estimation error to approximate the ranging error. With additive Gaussian white noise, the CRB of time delay estimation using TOA ranging is [11]

$$\sigma_{\varepsilon}^2 \geq \frac{1}{8\pi^2 \gamma \beta_f^2} \tag{4}$$

where σ_{ε}^2 is the variance of time delay estimation error, β_f is the bandwidth of ranging signal, and γ is signal-to-noise ratio (SNR). For omnidirectional antennas with only line-of-sight, we have

$$P_r = \frac{P}{4\pi d_{i,j}^2} \tag{5}$$

DOI: 10.1002/wcm

where P_r is received power, P is transmit power, and $d_{i,j}$ is the true distance between the transmitter (node i) and receiver (node j). When in a multipath channel, we have

$$P_r = \frac{P}{4\pi d_{i,j}^{2n}} \tag{6}$$

where n is *multipath factor* that depends on specific application scenarios.

The SNR of the received signal is

$$\gamma = \frac{P_r}{N_0 \beta_f} \tag{7}$$

where N_0 is the noise power spectral density. From Equations (4), (6), and (7), we can get

$$\sigma_\varepsilon^2 \geq \frac{N_0 d_{i,j}^{2n}}{2\pi\beta_f P} \tag{8}$$

Since our objective is to obtain the lower bound of ranging error, we take the equality in Equation (8) and multiply both sides with c^2 where c denotes the speed of light, and then we get

$$E\{(\hat{d}_{i,j} - d_{i,j})^2\} = c^2 \cdot \sigma_\varepsilon^2 = \frac{c^2 N_0 d_{i,j}^{2n}}{2\pi\beta_f P} \tag{9}$$

where $E\{\cdot\}$ means expectation. Similar to Reference [10], it is assumed that the ranging error follows a zero-mean normal distribution. Let $\sigma_0 = \sqrt{\frac{c^2 N_0}{2\pi\beta_f P}}$, then the ranging error model can be described as

$$\hat{d}_{i,j} = d_{i,j} + d_{i,j}^n \sigma_0 \varepsilon_0 \tag{10}$$

where σ_0 is defined as *noise factor*, and ε_0 is a standard normal random variable denoted as $\varepsilon_0 \sim N(0, 1)$.

2.3. Error Bound for Localization

With the ranging error model, the CRB for localization can be derived. Suppose there are (i) at least three anchor nodes (i.e., $N - M \geq 3$), and (ii) a sufficient number of measured distances between nodes in the WSN. Let

$$\boldsymbol{\theta}_n = (x_1, y_1, \cdots, x_M, y_M)^{\mathrm{T}} \tag{11}$$

be the coordinate vector of non-anchor nodes, and

$$\hat{\boldsymbol{\theta}}_n = (\hat{x}_1, \hat{y}_1, \cdots, \hat{x}_M, \hat{y}_M)^{\mathrm{T}} \tag{12}$$

be the estimated coordinate vector of non-anchor nodes. Then the error covariance matrix is

$$\mathbb{C} = E\{(\hat{\boldsymbol{\theta}}_n - \boldsymbol{\theta}_n)(\hat{\boldsymbol{\theta}}_n - \boldsymbol{\theta}_n)^{\mathrm{T}}\} \tag{13}$$

The error covariance matrix is bounded by the CRB, that is,

$$\mathbb{C} \geq \mathrm{CRB} \tag{14}$$

The CRB can be represented as

$$\mathrm{CRB} = \mathbb{J}^{-1} \tag{15}$$

where $\mathbb{J}$ is the Fisher Information Matrix (FIM). Note that the FIM has a full rank (and thus its inverse exists) only if there are at least three anchor nodes and a sufficient number of measured distances between nodes in the WSN. The method to obtain $\mathbb{J}$ in our model is described in details in the Appendix.

In an actual application, the location information provided by some anchor nodes may not be accurate. Still taking these anchor nodes as reference points will lead to inaccurate or even catastrophic results. Thus, we propose to first obtain the whole network's topology (i.e., a set of mutual distances of all the nodes) without use of anchor node location information, then detect and remove inaccurately positioned anchor nodes, and finally get the positions of all the nodes. So for the ranging error bound, we view the $N - M$ anchor nodes as non-anchor nodes, and thus have a $2N \times 2N$ FIM $\mathbb{J}$. Without anchor nodes, the FIM $\mathbb{J}$ has a rank of $2N - 3$ [9]. So the inverse of the FIM does not exist. This means lower bound of $E\{(\hat{x}_i - x_i)^2\}$ or $E\{(\hat{y}_i - y_i)^2\}$ for node i cannot be obtained. However, the lower bound of the summation of $E\{(\hat{x}_i - x_i)^2 + (\hat{y}_i - y_i)^2\}$, $i = 1, 2, \cdots, N$ can still be measured with the help of the rank-deficient FIM. According to References [9,12], $\sum_{i=1}^{N} E\{(\hat{x}_i - x_i)^2 + (\hat{y}_i - y_i)^2\}$ is no less than the trace (i.e., sum of diagonal elements) of $\mathbb{J}^\dagger$, where $\mathbb{J}^\dagger$ is the Moore–Penrose pseudo-inverse of $\mathbb{J}$. Let $\lambda_1, \lambda_2, \cdots, \lambda_{2N-3}$ be the non-zero eigenvalues of $\mathbb{J}$, then the trace of $\mathbb{J}^\dagger$ can be expressed as

$$Tr(\mathbb{J}^\dagger) = \sum_{i=1}^{2N-3} \frac{1}{\lambda_i} \tag{16}$$

Further, the average CRB of ranging errors can be obtained, given by $Tr(\mathbb{J}^\dagger)/N$.

DOI: 10.1002/wcm

3. Topology Reconstruction

3.1. Proposed Topology Reconstruction Method

To obtain a network topology, MDS [6] algorithm that only takes distance matrix as the input is a good candidate because of its capability of parallel computing. However, it requires that any pair of nodes should be able to reach each other, which is not practical. On the other hand, in Reference [13], a method is given for topology reconstruction from incomplete distance information. Let $\mathbb{D}$ be a distance matrix in which $\mathbb{D}_{i,j} = d_{i,j}^2$. It is proved in Reference [13] that the rank of $\mathbb{D}$ is at most 4. As discussed in Reference [13], suppose the first four rows of $\mathbb{D}$ are linearly independent and are known, which also means that each of the first 4 nodes can reach all other nodes. Also, assume that in each of other rows in $\mathbb{D}$, at least four entries are known, that is, each node can range the distance with at least four other nodes. Then the network topology can be reconstructed, that is, the value of each entry in $\mathbb{D}$ can be obtained. One problem in the topology reconstruction is how to find four nodes, each with measured distance to any other node. Furthermore, in the topology reconstruction method, it is assumed that $p_{i,j}$ (the probability that node i can measure the distance to node j) is known for any i and j. The assumption makes the method impractical in a real network. Another drawback of the topology reconstruction method comes from the fact that the accuracy of localization with the method depends largely on the 'best guess' of the distance between nodes i and j when the distance cannot be measured. In the following, we propose a new topology reconstruction method to solve these problems.

As aforementioned, it may be difficult to find four nodes in a WSN, each with measured distance to any other node. Generally, this condition can be satisfied in a local area, namely a sub-network. In other words, in the group of nodes in a sub-network, it is possible to find four nodes that can reach any other node in the group, and then to obtain the distance matrix of all nodes in the sub-network by the preceding procedure. Thus, the sub-network becomes *all-connected*, which means the distance between any pair of nodes is known. For a node in an adjacent area of the all-connected sub-network, if it can reach at least four nodes in the sub-network, its distance to any node in the sub-network can be obtained, and thus it can be included into the all-connected sub-network. This means the all-connected sub-network is gradually enlarged, and eventually it includes all the nodes in the WSN.

As ranging errors are inevitable, the performance of topology reconstruction can be degraded due to accumulated ranging errors. To deal with the error accumulation issue, we have the following requirements:

- The initially selected sub-network should be an all-connected sub-network rather than one with only four nodes that can reach any other node.
- Once adjacent nodes are included into the sub-network and new topology is generated (e.g., by MDS method), distance refinement is necessary to address the error accumulation in the search for adjacent nodes. We choose BFGS method [14] (a quasi-Newton method) to reduce the accumulated ranging errors.

Define a connection matrix as $\mathbb{W}$ in which $w_{i,j}$ is equal to 1 if the distance between node i and j is measurable and the measurement result is credible, and equal to 0 otherwise. The discovery mechanism to determine the $\mathbb{W}$ is as follows. In a sensor network, besides anchor nodes positions and mutual distance measurements, other information can also be obtained such as SNR or other parameters that can represent the credibility of ranging data between two nodes [15]. The ranging data is accepted if its credibility is high, and discarded otherwise.

Our topology reconstruction method is stated as follows.

Step 1: *Setup of initial all-connected sub-network*—Set $k = 0$, find an all-connected sub-network $\mathcal{A}_k$, in which $|\mathcal{A}_k| \geq 4$, that is, the number of elements in set $\mathcal{A}_k$ is not less than 4, and generate distance matrix $\mathbb{D}_0$ for the sub-network.[‡]

Step 2: *Inclusion of new adjacent nodes*—According to connection matrix $\mathbb{W}$, search the set $\mathcal{B}_k = \{i | i \notin \mathcal{A}_k, |\mathcal{F}(i) \cap \mathcal{A}_k| \geq 4\}$, that is, each node in $\mathcal{B}_k$ has at least four measured distances with nodes in $\mathcal{A}_k$. All the nodes in $\mathcal{B}_k$ are to

[‡] It is possible that the initial four fully connected nodes are not able to be found. However, for a localization problem with TOA technique in a 2D plane, one basic requirement for each node is that it can communicate with at least three other nodes. Considering the basic requirement, the worst case (i.e., the initial four fully connected nodes cannot be found) happens only when all the nodes are sparsely and evenly located in the network. So the probability of the worst case is expected to be low.

DOI: 10.1002/wcm

be added into the all-connected network $\mathcal{A}_k$, shown as follows.

For each $i \in \mathcal{B}_k$, define $\mathcal{T}_i$ as the set of nodes in $\mathcal{A}_k$ that have measured distances with i, denoted as $\mathcal{T}_i = \{j | j \in \mathcal{F}(i) \cap \mathcal{A}_k\}$. Obviously, $|\mathcal{T}_i| \geq 4$. Let $\mathcal{R}_i = \mathcal{A}_k \backslash \mathcal{T}_i$. So we need to know the distances of i to the nodes in $\mathcal{R}_i$. Without loss of generality, we assume $|\mathcal{A}_k| = m$, $|\mathcal{T}_i| = l \geq 4$, the nodes in $\mathcal{T}_i$ are with IDs from 1 to l, and nodes in $\mathcal{R}_i$ are with IDs from $l+1$ to m. So the distance matrix of the set $\mathcal{A}_k \cup \{i\}$ is given by

$$\mathbb{D}_k = \begin{pmatrix} \hat{d}_{1,1}^2 & \hat{d}_{1,2}^2 & \cdots & \hat{d}_{1,m}^2 & \hat{d}_{1,i}^2 \\ \vdots & \vdots & \ddots & \vdots & \vdots \\ \hat{d}_{l,1}^2 & \hat{d}_{l,2}^2 & \cdots & \hat{d}_{l,m}^2 & \hat{d}_{l,i}^2 \\ \vdots & \vdots & \ddots & \vdots & \vdots \\ \hat{d}_{m,1}^2 & \hat{d}_{m,2}^2 & \cdots & \hat{d}_{m,m}^2 & \hat{d}_{m,i}^2 \\ \hat{d}_{i,1}^2 & \hat{d}_{i,2}^2 & \cdots & \hat{d}_{i,m}^2 & \hat{d}_{i,i}^2 \end{pmatrix}$$

All the diagonal entries are 0s. The unknown entries in $\mathbb{D}_k$ are $\hat{d}_{i,l+1}^2, \hat{d}_{i,l+2}^2, \cdots, \hat{d}_{i,m}^2$.[§] Because the rank of $\mathbb{D}$ is at most 4 and $l \geq 4$, the last row in $\mathbb{D}_k$ can be represented by a linear combination of the first l rows, that is,

$$\begin{pmatrix} \hat{d}_{1,1}^2 & \hat{d}_{2,1}^2 & \cdots & \hat{d}_{l,1}^2 \\ \hat{d}_{1,2}^2 & \hat{d}_{2,2}^2 & \cdots & \hat{d}_{l,2}^2 \\ \vdots & \vdots & \ddots & \vdots \\ \hat{d}_{1,m}^2 & \hat{d}_{2,m}^2 & \cdots & \hat{d}_{l,m}^2 \\ \hat{d}_{1,i}^2 & \hat{d}_{2,i}^2 & \cdots & \hat{d}_{l,i}^2 \end{pmatrix} \begin{pmatrix} c_1 \\ c_2 \\ \vdots \\ c_l \end{pmatrix} = \begin{pmatrix} \hat{d}_{i,1}^2 \\ \hat{d}_{i,2}^2 \\ \vdots \\ \hat{d}_{i,m}^2 \\ \hat{d}_{i,i}^2 \end{pmatrix} \tag{17}$$

From Equation (17), we can obtain the values of $c_1, c_2, \cdots, c_l$, and further get the values of $\hat{d}_{i,l+1}^2, \hat{d}_{i,l+2}^2, \cdots, \hat{d}_{i,m}^2$.

Step 3: *Topology refinement*—After all nodes in $\mathcal{B}_k$ are added into $\mathcal{A}_k$, use MDS method on the present $\mathbb{D}_k$ (for nodes in the present $\mathcal{A}_k$) to get the estimated coordinate vectors of nodes in $\mathcal{A}_k$ (e.g., $(\hat{x}_i, \hat{y}_i)$ for node i). Then use the BFGS method to adjust the coordinate vectors of the nodes such that the following objective function

$$\sum_{i<j, j\in\mathcal{F}(i), i\in\mathcal{A}_k, j\in\mathcal{A}_k} \left(\hat{d}_{i,j} - \sqrt{(\hat{x}_i - \hat{x}_j)^2 + (\hat{y}_i - \hat{y}_j)^2}\right)^2 \tag{18}$$

is minimized. And update entries of $\mathbb{D}_k$ accordingly.

Step 4: Increase k by 1, and proceed to Step 2 until all the nodes in the WSN have been included in $\mathcal{A}_k$.

3.2. Analysis of the Proposed Topology Reconstruction Method

In the proposed topology reconstruction method, the main operation includes the hierarchical update of topology reconstruction in Step 2, and MDS method and BFGS method in Step 3. The feature how the MDS method and BFGS method address the ranging error can be found in References [16] and [14], respectively. In the following, we will analyze the hierarchical update of the topology reconstruction. Let

$$\mathbb{A}_1 + \Delta\mathbb{A}_1 = \begin{pmatrix} \hat{d}_{1,1}^2 & \hat{d}_{2,1}^2 & \cdots & \hat{d}_{l,1}^2 \\ \hat{d}_{1,2}^2 & \hat{d}_{2,2}^2 & \cdots & \hat{d}_{l,2}^2 \\ \vdots & \vdots & \ddots & \vdots \\ \hat{d}_{1,l}^2 & \hat{d}_{2,l}^2 & \cdots & \hat{d}_{l,l}^2 \\ \hat{d}_{1,i}^2 & \hat{d}_{2,i}^2 & \cdots & \hat{d}_{l,i}^2 \end{pmatrix}$$

where $\mathbb{A}_1$ denotes the true distance matrix and $\Delta\mathbb{A}_1$ denotes the distance error matrix. We also define

$$\boldsymbol{b}_1 + \Delta\boldsymbol{b}_1 = \left(\hat{d}_{i,1}^2, \hat{d}_{i,2}^2, \cdots, \hat{d}_{i,l}^2, \hat{d}_{i,i}^2\right)^{\mathrm{T}}$$

where $\boldsymbol{b}_1$ denotes the true distance vector and $\Delta\boldsymbol{b}_1$ denotes the distance error vector,

$$\mathbb{A}_2 + \Delta\mathbb{A}_2 = \begin{pmatrix} \hat{d}_{1,l+1}^2 & \hat{d}_{2,l+1}^2 & \cdots & \hat{d}_{l,l+1}^2 \\ \hat{d}_{1,l+2}^2 & \hat{d}_{2,l+2}^2 & \cdots & \hat{d}_{l,l+2}^2 \\ \vdots & \vdots & \ddots & \vdots \\ \hat{d}_{1,m}^2 & \hat{d}_{2,m}^2 & \cdots & \hat{d}_{l,m}^2 \end{pmatrix}$$

$$\boldsymbol{b}_2 + \Delta\boldsymbol{b}_2 = \left(\hat{d}_{i,l+1}^2, \hat{d}_{i,l+2}^2, \cdots, \hat{d}_{i,m}^2\right)^{\mathrm{T}}$$

[§] Since $\mathbb{D}$ is a symmetric matrix, we do not count the unknown entries $\hat{d}_{l+1,i}^2, \hat{d}_{l+2,i}^2, \cdots, \hat{d}_{m,i}^2$.

DOI: 10.1002/wcm

and

$$\boldsymbol{c} = (c_1, c_2, \cdots, c_l)^{\mathrm{T}} \tag{19}$$

Obviously, we have

$$\mathbb{A}_1\boldsymbol{c} = \boldsymbol{b}_1 \tag{20}$$

$$\mathbb{A}_2\boldsymbol{c} = \boldsymbol{b}_2 \tag{21}$$

and

$$\boldsymbol{b}_1 + \Delta\boldsymbol{b}_1 = (\mathbb{A}_1 + \Delta\mathbb{A}_1)(\boldsymbol{c} + \Delta\boldsymbol{c}) \tag{22}$$

$$\boldsymbol{b}_2 + \Delta\boldsymbol{b}_2 = (\mathbb{A}_2 + \Delta\mathbb{A}_2)(\boldsymbol{c} + \Delta\boldsymbol{c}) \tag{23}$$

To minimize the estimation error of $\boldsymbol{b}_2$, we can state the object as

$$\text{minimize}\|\Delta\boldsymbol{b}_2\| \tag{24}$$

where $\|\cdot\|$ means the L^2-norm of a vector, that is, $\|(x_1, x_2, \cdots, x_n)^{\mathrm{T}}\| = \sqrt{x_1^2 + x_2^2 + \cdots + x_n^2}$. From Equations (21) and (23), we can derive that

$$\Delta\boldsymbol{b}_2 = \Delta\mathbb{A}_2\boldsymbol{c} + (\mathbb{A}_2 + \Delta\mathbb{A}_2)\Delta\boldsymbol{c} \tag{25}$$

So it is desired to minimize $\|\Delta\mathbb{A}_2\boldsymbol{c} + (\mathbb{A}_2 + \Delta\mathbb{A}_2)\Delta\boldsymbol{c}\|$, which is equivalent to solving the following equation that is very likely to be an inconsistent equation:

$$-(\mathbb{A}_2 + \Delta\mathbb{A}_2)\Delta\boldsymbol{c} = \Delta\mathbb{A}_2\boldsymbol{c} \tag{26}$$

According to Reference [17], the best solution to minimize $\|\Delta\mathbb{A}_2\boldsymbol{c} + (\mathbb{A}_2 + \Delta\mathbb{A}_2)\Delta\boldsymbol{c}\|$ should be

$$\Delta\boldsymbol{c} = -\left((\mathbb{A}_2 + \Delta\mathbb{A}_2)^{\mathrm{T}}(\mathbb{A}_2 + \Delta\mathbb{A}_2)\right)^{-1} (\mathbb{A}_2 + \Delta\mathbb{A}_2)^{\mathrm{T}}\Delta\mathbb{A}_2\boldsymbol{c} \tag{27}$$

However, since $\Delta\mathbb{A}_2$ is unknown, it may not be feasible to design a method to get the best estimation of $\boldsymbol{b}_2$ based on Equation (27). Therefore, we alternatively aim at estimating $\boldsymbol{c}$ as accurately as possible, and our goal can then be formulated as

$$\text{minimize}\|(\mathbb{A}_1+\Delta\mathbb{A}_1)(\boldsymbol{c}+\Delta\boldsymbol{c})-(\boldsymbol{b}_1+\Delta\boldsymbol{b}_1)\| \tag{28}$$

Similar to Equation (27), the best solution is

$$\hat{\boldsymbol{c}} = \left((\mathbb{A}_1 + \Delta\mathbb{A}_1)^{\mathrm{T}}(\mathbb{A}_1 + \Delta\mathbb{A}_1)\right)^{-1} (\mathbb{A}_1 + \Delta\mathbb{A}_1)^{\mathrm{T}}(\boldsymbol{b}_1 + \Delta\boldsymbol{b}_1) \tag{29}$$

which is exactly what we use to solve Equation (17) in Step 2 of our proposed topology reconstruction.

Next, we explain the reason why we use a linear combination of the first l rows in $\mathbb{D}_k$ to represent the last row. Since the rank of matrix $[\mathbb{A}_1^{\mathrm{T}}\ \mathbb{A}_2^{\mathrm{T}}]$ is at most 4 [13], one may guess that it is sufficient to use only four rows in $\mathbb{D}_k$ to represent the last row. However, $\mathbb{A}_1$ is disturbed by $\Delta\mathbb{A}_1$. To address estimation error, that is, $\Delta\mathbb{A}_1$, we use all the first l rows in $\mathbb{D}_k$ to represent the last row. Denote $\widetilde{\mathbb{A}} = \mathbb{A}_1 + \Delta\mathbb{A}_1$ and $\widetilde{\boldsymbol{b}} = \boldsymbol{b}_1 + \Delta\boldsymbol{b}_1$. Let $\widetilde{\mathbb{S}A}$ be a $(l+1) \times j$ ($j \leq l$) matrix whose columns are selected from columns of $\widetilde{\mathbb{A}}$. Then, we have

$$\|\widetilde{\mathbb{A}}\left(\widetilde{\mathbb{A}}^{\mathrm{T}}\widetilde{\mathbb{A}}\right)^{-1}\widetilde{\mathbb{A}}^{\mathrm{T}}\widetilde{\boldsymbol{b}} - \widetilde{\boldsymbol{b}}\| \leq \|\widetilde{\mathbb{S}A}\left(\widetilde{\mathbb{S}A}^{\mathrm{T}}\widetilde{\mathbb{S}A}\right)^{-1}\widetilde{\mathbb{S}A}^{\mathrm{T}}\widetilde{\boldsymbol{b}} - \widetilde{\boldsymbol{b}}\| \tag{30}$$

as proved as follows.

Proof. $\left(\widetilde{\mathbb{A}}^{\mathrm{T}}\widetilde{\mathbb{A}}\right)^{-1}\widetilde{\mathbb{A}}^{\mathrm{T}}\widetilde{\boldsymbol{b}}$ is the optimal solution to minimize $\|\widetilde{\mathbb{A}}\boldsymbol{x} - \widetilde{\boldsymbol{b}}\|$ [17], that is, for arbitrary vector $\boldsymbol{x} = (x_1, x_2, \cdots, x_l)^{\mathrm{T}}$, we have

$$\|\widetilde{\mathbb{A}}\left(\widetilde{\mathbb{A}}^{\mathrm{T}}\widetilde{\mathbb{A}}\right)^{-1}\widetilde{\mathbb{A}}^{\mathrm{T}}\widetilde{\boldsymbol{b}} - \widetilde{\boldsymbol{b}}\| \leq \|\widetilde{\mathbb{A}}\boldsymbol{x} - \widetilde{\boldsymbol{b}}\| \tag{31}$$

Let $\boldsymbol{x} = \widetilde{\mathbb{B}}\left(\widetilde{\mathbb{S}A}^{\mathrm{T}}\widetilde{\mathbb{S}A}\right)^{-1}\widetilde{\mathbb{S}A}^{\mathrm{T}}\widetilde{\boldsymbol{b}}$ where $\widetilde{\mathbb{B}}$ satisfies $\widetilde{\mathbb{A}}\widetilde{\mathbb{B}} = \widetilde{\mathbb{S}A}$. From Equation (31), we can get

$$\begin{aligned}\left\|\widetilde{\mathbb{A}}\left(\widetilde{\mathbb{A}}^{\mathrm{T}}\widetilde{\mathbb{A}}\right)^{-1}\widetilde{\mathbb{A}}^{\mathrm{T}}\widetilde{\boldsymbol{b}} - \widetilde{\boldsymbol{b}}\right\| &\leq \left\|\widetilde{\mathbb{A}}\widetilde{\mathbb{B}}\left(\widetilde{\mathbb{S}A}^{\mathrm{T}}\widetilde{\mathbb{S}A}\right)^{-1}\widetilde{\mathbb{S}A}^{\mathrm{T}}\widetilde{\boldsymbol{b}} - \boldsymbol{b}\right\| \\ &= \left\|\widetilde{\mathbb{S}A}\left(\widetilde{\mathbb{S}A}^{\mathrm{T}}\widetilde{\mathbb{S}A}\right)^{-1}\widetilde{\mathbb{S}A}^{\mathrm{T}}\widetilde{\boldsymbol{b}} - \widetilde{\boldsymbol{b}}\right\|\end{aligned} \tag{32}$$

This completes the proof. ■

So it is clear that using more rows in $\mathbb{D}_k$ to represent the last row will promise less estimation error.

4. Detection of Inaccurately Positioned Anchor Nodes

Once the network topology is reconstructed (as discussed in the previous section), the positions of all non-anchor nodes can be obtained based on the reconstructed network topology and known anchor node positions. However, since some anchor nodes may be inaccurately positioned, it is necessary to detect these anchor nodes and prevent them from serving as reference nodes. Note that the inaccurately positioned anchor nodes are still able to measure the distances to

DOI: 10.1002/wcm

their neighboring nodes and broadcast them correctly. So the reconstructed network topology is assumed to be accurate because the position information of anchor nodes is not used in the reconstruction procedure. It is also assumed that only a small portion of the anchor nodes are inaccurately positioned, and their position errors are randomly distributed.

Define a matrix $\mathbb{U}$ in which an entry $u_{i,j}$ means the *estimated distance* (in the topology reconstruction) of anchor node i to anchor node j, that is, $\hat{d}_{i,j}$. Define a matrix $\mathbb{V}$ in which an entry $v_{i,j}$ means the *declared distance* of anchor node i to anchor node j, that is, the distance calculated based on the position information broadcast from the anchor nodes. Also define a difference matrix $\mathbb{Q}$ in which

$$q_{i,j} = \begin{cases} 1, & \text{if } \frac{|u_{i,j}-v_{i,j}|}{u_{i,j}} < \tau \\ 0, & \text{otherwise} \end{cases} \tag{33}$$

where τ is a pre-specified threshold. It can be seen that the more the position error of an anchor node i, the larger the likelihood of $q_{i,j}$ (with another anchor node j) being 0. Note that for an inaccurately positioned anchor node i, the $q_{i,j}$s may not be all 0s. Therefore, in order to detect inaccurately positioned anchor nodes, we propose to find the set of accurately positioned anchor nodes instead, as described in the following. The principle in the detection of accurately positioned anchor nodes is the fact that $q_{i,j}$ should be 1 if anchor nodes i and j are both accurately positioned. For the simplicity of presentation, if $q_{i,j} = 1$, we say anchor nodes i and j are connected. Thus, our objective is to find the maximum set of all-connected anchor nodes. This can be achieved by a heuristic method, that is, first getting a small set of all-connected anchor nodes and then gradually adding new anchor nodes into the set until no more new anchor nodes can be added. The detailed procedure is stated as follows.

Step 1: Find all pairs of connected anchor nodes. Each pair is an all-connected set.
Step 2: For each all-connected set, if any other anchor node is connected to all of its element nodes, include the anchor node into the set and form an enlarged all-connected set. This procedure is continued until no new anchor node can be included in the set.
Step 3: The all-connected set with the largest number of elements is our objective result.

Once the set of accurately positioned anchor nodes is obtained, the locations of non-anchor nodes and inaccurately positioned anchor nodes can be calculated based on the reconstructed network topology and the locations of the accurately positioned anchor nodes, using a method similar to that in Reference [12].

Currently, the proposed algorithm (including topology reconstruction and inaccurately positioned anchor node detection methods) is performed in a central controller. For a large WSN, it is desired to perform localization in a distributed mode. In this case, we can use a solution similar to that in Reference [6]. The WSN can be partitioned into sub-networks. In each sub-network, our proposed algorithm can be performed in a local central controller. Then the maps of the local sub-networks can be merged to form the map of the whole WSN.

5. Performance Evaluation

We evaluate the performance of our proposed algorithm through simulations. A number $N = 100$ nodes are randomly placed in a unit square. The multipath factor n is assumed to be 1.

5.1. Evaluation of Topology Reconstruction

We use root mean square distance (RMSD) [2] to measure estimation error

$$\text{RMSD} = \frac{1}{\sqrt{N}} \sqrt{\sum_{i=1}^{N} \left((x_i - \hat{x}_i)^2 + (y_i - \hat{y}_i)^2 \right)} \tag{34}$$

5.1.1. Effect of refinement steps

Figure 1 shows the relationship between estimation error (RMSD^2) and the number of search steps in BFGS method. Noise factor σ_0 is 0.3, and visible radius R is 0.6. As the figure reveals, estimation error becomes almost stable when the number of search steps is larger than 15. So we choose 15 as default number of search steps for subsequent simulations.

5.1.2. Effect of noise factor

Figure 2 shows the estimation error when the noise factor σ_0 increases from 0.05 to 0.4. In the simulation, visible radius is set to be 0.5. It can be seen that the estimation error increases with the noise factor. The average CRB as derived in Section 2 (i.e., $Tr(\mathbb{J}^{\dagger})/N$) is also shown in Figure 2 for comparison.

DOI: 10.1002/wcm

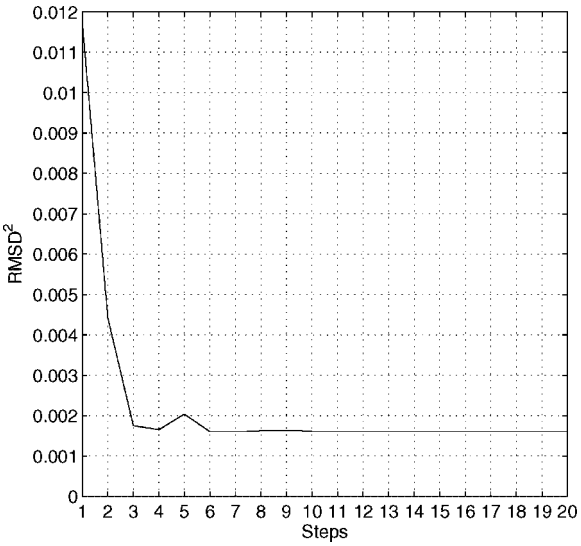

Fig. 1. Estimation error *versus* the number of search steps using BFGS method.

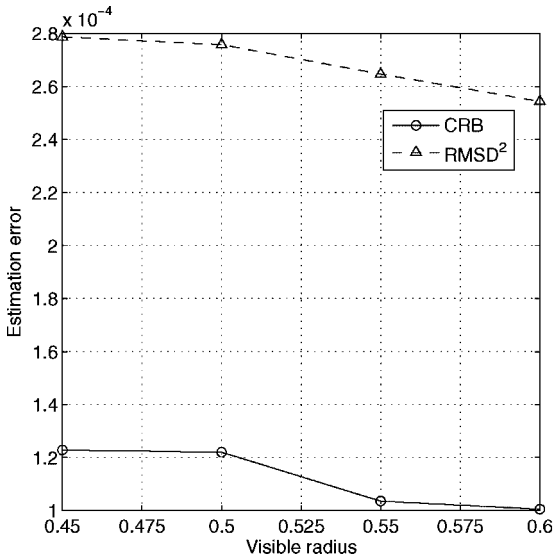

Fig. 3. Estimation error *versus* visible radius.

The result demonstrates that the estimation error in our method can keep two to three times corresponding CRB. This result is reasonable as explained in the following.

The optimization problem for localization has been shown to be a non-convex problem [12,18]. So for traditional numerical methods, only local optimization can be achieved. Thus, it is reasonable that the estimation error in our method keeps two to three times CRB. Although global optimization methods such as genetic algorithm [19] or simulated annealing algorithm [20] can be implemented, the computation complexity is very high, which may not be desired in WSNs.

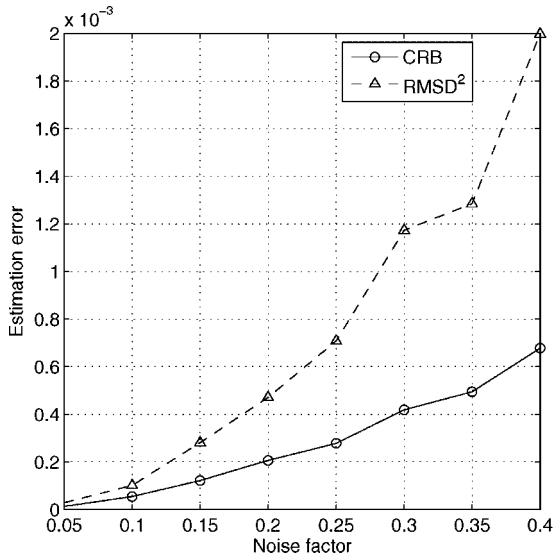

Fig. 2. Estimation error *versus* noise factor.

5.1.3. Effect of visible radius

Figure 3 shows the estimation error when the visible radius varies from 0.45 to 0.6. Noise factor is set to be 0.15. It can be seen that the estimation error in our proposed method can keep about 2.5 times CRB. When the visible radius increases, the estimation error decreases. This is because with a larger visible radius, more pairs of nodes can have measured distance, thus enhancing the localization accuracy.

5.2. Evaluation of Inaccurately Positioned Anchor Node Detection

We first show the comparison of our inaccurately positioned anchor node detection with Multilateration [5] and our topology reconstruction algorithm in Section 3 without inaccurately positioned anchor node detection. In the simulations, noise factor is fixed at 0.2, visible radius is 0.5, the number of anchor nodes is 10 (with IDs from 1 to 10), and 3 of them (with IDs from 1 to 3) are inaccurately positioned. Figure 4 shows the true positions and estimated positions with different algorithms. True location of a node is marked by an asterisk. For an inaccurately positioned anchor node, the broadcast location (i.e., the false location) is marked

DOI: 10.1002/wcm

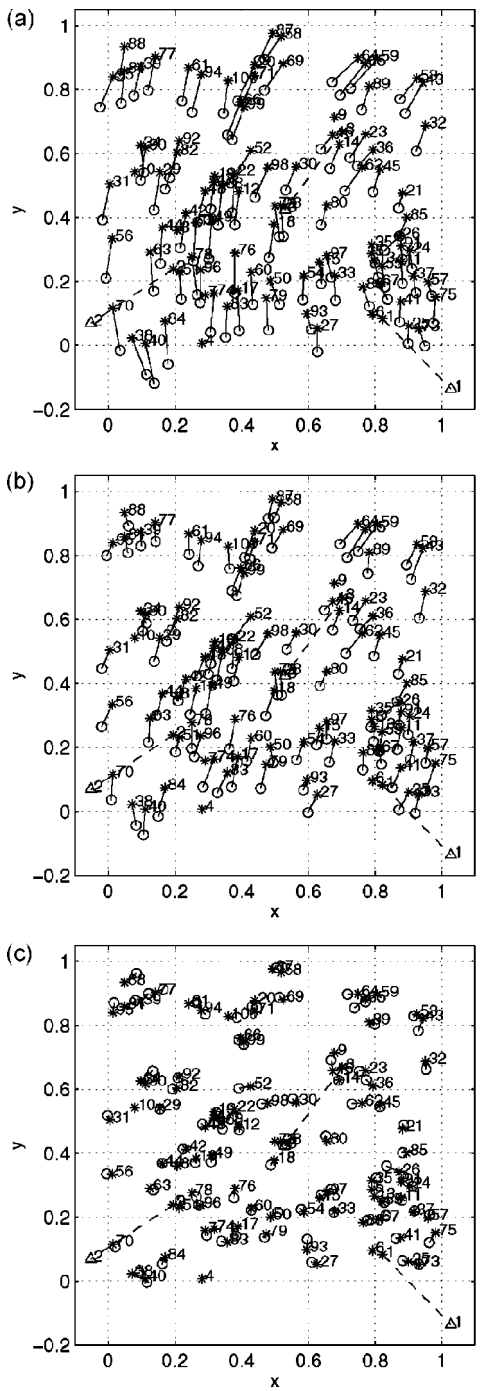

Fig. 4. A comparison between Multilateration algorithm and our topology reconstruction algorithm without and with inaccurately positioned anchor node detection. (a) Localization result of Multilateration algorithm. (b) Localization result of our topology reconstruction algorithm without inaccurately positioned anchor node detection. (c) Localization result of our topology reconstruction algorithm with inaccurately positioned anchor node detection.

by a triangle, and is connected with the true location by a dashed line. For a non-anchor node, the estimated location is marked by a circle, and is connected with the true location by a solid line. The RMSD of non-anchor nodes in Figure 4(a), (b), and (c) is 0.0967, 0.0701, and 0.0218, respectively. It can be seen that our inaccurately positioned anchor node detection can improve the accuracy of localization.

The value of threshold τ is critical in the inaccurately positioned anchor node detection. If the threshold is too low, some entries in $\mathbb{Q}$ that should be 1 will be marked as 0, then accurately positioned anchor nodes will be mistaken for inaccurately positioned anchor nodes; if the threshold is too high, it is possible that some inaccurately positioned anchor nodes will be mistaken for accurately positioned anchor nodes. Figure 5(a), (b), and (c) show the effective interval[‖] (lower bound and upper bound) of τ when there is one inaccurately positioned anchor node and the *offset distance* (the distance between true location and broadcast (false) location of the inaccurately positioned anchor node) is 0.3, 0.4, and 0.5, respectively. Figure 6 shows the result when the number of inaccurately positioned anchor nodes is 3. It can be seen that:

- When the offset distance becomes larger with a fixed noise factor, the upper bound of τ increases while the lower bound almost keeps constant.
- When the noise factor becomes larger with a fixed offset distance, lower bound of τ increases while the upper bound only fluctuates slightly.

These can be explained as follows. When the noise factor grows, the estimation error level will grow as well, and so do the entries $\frac{|u_{i,j}-v_{i,j}|}{u_{i,j}}$. To avoid false detection of inaccurately positioned anchor nodes, the lower bound of τ should also become larger. In other words, lower bound of τ is mainly determined by noise factor. On the other hand, a larger offset distance can make inaccurately positioned anchor nodes be easier to be detected, thus leading to a higher upper bound of τ. This means the upper bound of τ is primarily determined by offset distance.

Simulation results also show that there is a broad interval for selection of threshold τ in our inaccurately positioned anchor node detection.

[‖] A τ value in the effective interval can achieve effective detection of inaccurately positioned anchor nodes.

DOI: 10.1002/wcm

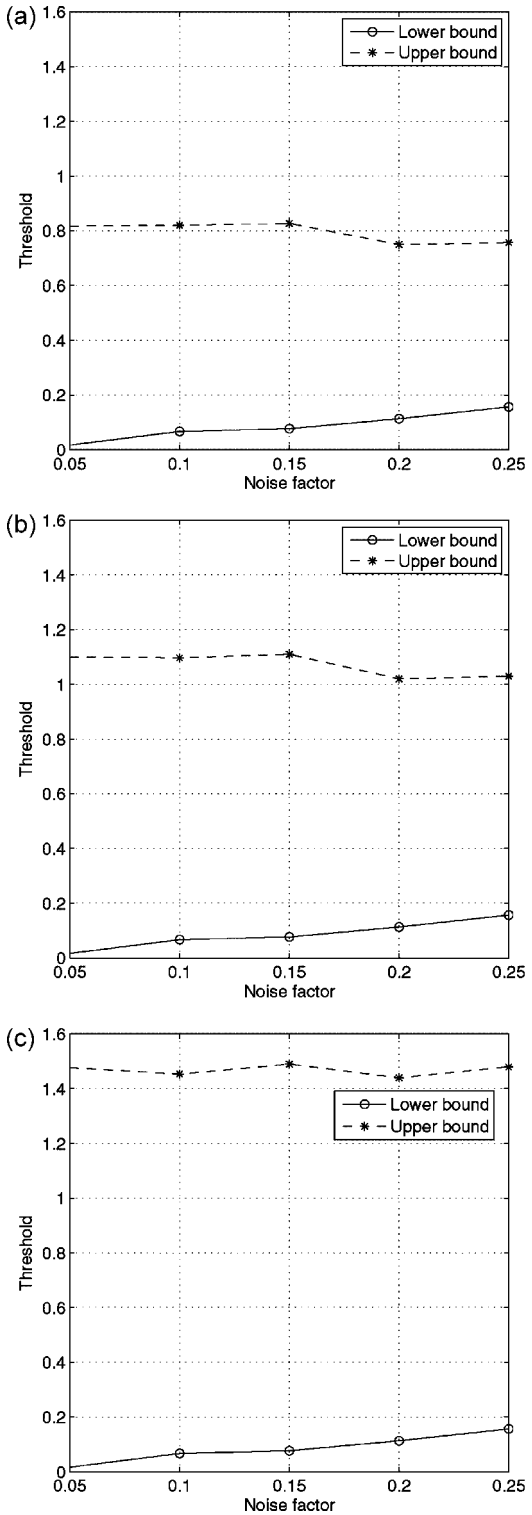

Fig. 5. Effective interval of τ *versus* noise factor with one inaccurately positioned anchor node. (a) Offset distance is 0.3. (b) Offset distance is 0.4. (c) Offset distance is 0.5.

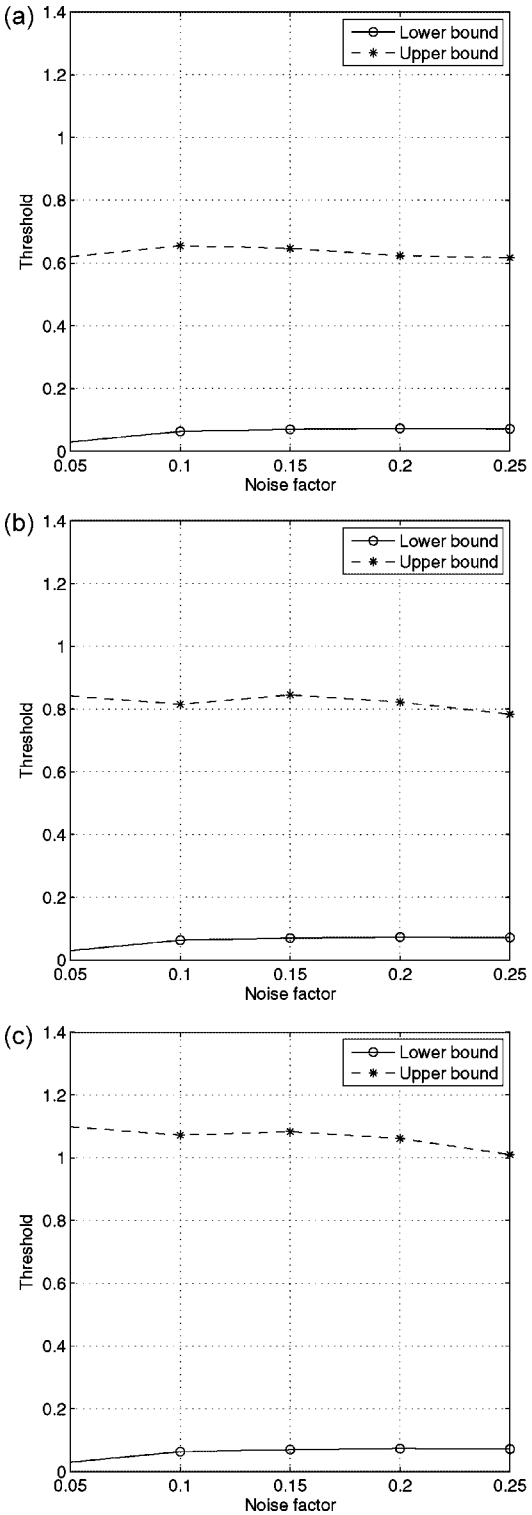

Fig. 6. Effective interval of τ *versus* noise factor with three inaccurately positioned anchor nodes. (a) Offset distance is 0.3. (b) Offset distance is 0.4. (c) Offset distance is 0.5.

DOI: 10.1002/wcm

6. Conclusions and Further Discussions

In this paper, to measure localization accuracy in WSNs, we first present a ranging error model for TOA estimation, and derive CRB for localization accordingly. Ranging error resistance and reference location error tolerance are two challenging tasks in localization. We address these issues by a topology reconstruction method without use of anchor node location information and a method to detect inaccurately positioned anchor nodes. Simulation results show that the estimation error in our proposed topology reconstruction method can maintain two to three times CRB, and inaccurately positioned anchor node detection method can improve localization accuracy significantly.

Currently, we consider a WSN with Gaussian distance measurement errors. On the other hand, in many cases, non-Gaussian distance measurement errors exist. Interesting issues for future work may include derivation of the lower bound of non-Gaussian distance measurement errors, based on existing [3] or emerging non-Gaussian error model. Since the analysis is much more challenging than that with Gaussian errors, significant research efforts are needed.

Appendix : Derivation of $\mathbb{J}$

According to deduced ranging error model in Subsection 2.2, it can be proved that

$$\mathbb{J}_{2i-1,2i-1} = \sum_{j\in F(i)} \left(\frac{2n^2(x_i - x_j)^2}{d_{i,j}^4} + \frac{1}{\sigma_0^2} \cdot \frac{(x_i - x_j)^2}{d_{i,j}^{2n+2}} \right) \tag{35}$$

$$\mathbb{J}_{2i,2i} = \sum_{j\in F(i)} \left(\frac{2n^2(y_i - y_j)^2}{d_{i,j}^4} + \frac{1}{\sigma_0^2} \cdot \frac{(y_i - y_j)^2}{d_{i,j}^{2n+2}} \right) \tag{36}$$

$$\mathbb{J}_{2i,2i-1} = \mathbb{J}_{2i-1,2i} = \sum_{j\in F(i)} \left(\frac{2n^2(x_i - x_j)(y_i - y_j)}{d_{i,j}^4} + \frac{1}{\sigma_0^2} \cdot \frac{(x_i - x_j)(y_i - y_j)}{d_{i,j}^{2n+2}} \right) \tag{37}$$

For $j \neq i$, if $j \in F(i)$

$$\mathbb{J}_{2i-1,2j-1} = \mathbb{J}_{2j-1,2i-1} = -\left(\frac{2n^2(x_i - x_j)^2}{d_{i,j}^4} + \frac{1}{\sigma_0^2} \cdot \frac{(x_i - x_j)^2}{d_{i,j}^{2n+2}} \right) \tag{38}$$

$$\mathbb{J}_{2i,2j} = \mathbb{J}_{2j,2i} = -\left(\frac{2n^2(y_i - y_j)^2}{d_{i,j}^4} + \frac{1}{\sigma_0^2} \cdot \frac{(y_i - y_j)^2}{d_{i,j}^{2n+2}} \right) \tag{39}$$

$$\mathbb{J}_{2i-1,2j} = \mathbb{J}_{2j,2i-1} = \mathbb{J}_{2i,2j-1} = \mathbb{J}_{2j-1,2i} = -\left(\frac{2n^2(x_i - x_j)(y_i - y_j)}{d_{i,j}^4} + \frac{1}{\sigma_0^2} \cdot \frac{(x_i - x_j)(y_i - y_j)}{d_{i,j}^{2n+2}} \right) \tag{40}$$

Other entries in $\mathbb{J}$ are 0s.

Proof. Let $\boldsymbol{x}$ and $\boldsymbol{y}$ be the vector of x-coordinates and y-coordinates of all the nodes, respectively. Let $\hat{\boldsymbol{d}}$ be the vector of measured distances (e.g., $\hat{d}_{i,j}$ from node i to node j) in the network. We first have the probability density function (PDF) of $\hat{\boldsymbol{d}}$ conditioned on $\boldsymbol{x}$ and $\boldsymbol{y}$ as follows:

$$p(\hat{\boldsymbol{d}}|\boldsymbol{x}, \boldsymbol{y}) = \prod_{i<j, j\in F(i)} \frac{\mathrm{e}^{-(\hat{d}_{i,j} - d_{i,j})^2/2\sigma_0^2 d_{i,j}^{2n}}}{\sqrt{2\pi}\sigma_0 d_{i,j}^n} \tag{41}$$

So the Log-likelihood function of $p(\hat{\boldsymbol{d}}|\boldsymbol{x}, \boldsymbol{y})$ is given by

$$\ln p(\hat{\boldsymbol{d}}|\boldsymbol{x}, \boldsymbol{y}) = C - \sum_{i<j, j\in F(i)} \left(\ln d_{i,j}^n + \frac{1}{2\sigma_0^2} \frac{(\hat{d}_{i,j} - d_{i,j})^2}{d_{i,j}^{2n}} \right) \tag{42}$$

where C is a constant. Take first-order and second-order partial derivative of $\ln p(\hat{\boldsymbol{d}}|\boldsymbol{x}, \boldsymbol{y})$ with respect to x_i, we have

$$\frac{\partial \ln p(\hat{\boldsymbol{d}}|\boldsymbol{x}, \boldsymbol{y})}{\partial x_i} = -\sum_{j\in F(i)} \left(\frac{n}{d_{i,j}} + \frac{1}{\sigma_0^2} \left(d_{i,j}^{-(n-1)} - \frac{\hat{d}_{i,j}}{d_{i,j}^n} \right) \cdot \left(\frac{n\hat{d}_{i,j}}{d_{i,j}^{n+1}} - \frac{(n-1)}{d_{i,j}^n} \right) \right) \cdot \frac{(x_i - x_j)}{d_{i,j}} \tag{43}$$

DOI: 10.1002/wcm

$$\frac{\partial^2 \ln p(\hat{\boldsymbol{d}}|\boldsymbol{x}, \boldsymbol{y})}{\partial x_i^2} = -\sum_{j\in F(i)} \left(\frac{n(d_{i,j}^2 - 2(x_i - x_j)^2)}{d_{i,j}^4} + \frac{n\hat{d}_{i,j}}{\sigma_0^2} \cdot \frac{(d_{i,j}^2 - (2n+1)(x_i - x_j)^2)}{d_{i,j}^{2n+3}} - \frac{n-1}{\sigma_0^2} \cdot \frac{(d_{i,j}^2 - 2n(x_i - x_j)^2)}{d_{i,j}^{2n+2}} - \frac{n\hat{d}_{i,j}^2}{\sigma_0^2} \cdot \frac{(d_{i,j}^2 - 2(n+1)(x_i - x_j)^2)}{d_{i,j}^{2n+4}} + \frac{(n-1)\hat{d}_{i,j}}{\sigma_0^2} \cdot \left(\frac{d_{i,j}^2 - (2n+1)(x_i - x_j)^2}{d_{i,j}^{2n+3}} \right) \right) \quad (44)$$

Because

$$E\{\hat{d}_{i,j}\} = d_{i,j} \quad (45)$$

$$E\{\hat{d}_{i,j}^2\} = d_{i,j}^2 + d_{i,j}^{2n} \cdot \sigma_0^2 \quad (46)$$

we can get the $(2i-1, 2i-1)$th entry of $\mathbb{J}$ as

$$\mathbb{J}_{2i-1,2i-1} = -E\left\{ \frac{\partial^2 \ln p(\hat{\boldsymbol{d}}|\boldsymbol{x}, \boldsymbol{y})}{\partial x_i^2} \right\} = \sum_{j\in F(i)} \left(\frac{2n^2(x_i - x_j)^2}{d_{i,j}^4} + \frac{1}{\sigma_0^2} \cdot \frac{(x_i - x_j)^2}{d_{i,j}^{2n+2}} \right) \quad (47)$$

Other entries of $\mathbb{J}$ can be obtained similarly. This completes the proof. ■

References

1. He T, Huang C, Blum BM, Stankovic JA, Abdelzaher T. Range-free localization schemes for large scale sensor networks. In *Proceedings of ACM MobiCom* 2003; 81–95.
2. Biswas P, Liang T-C, Toh K-C, Ye Y, Wang T-C. Semidefinite programming approaches for sensor network localization with noisy distance measurements. *IEEE Transactions on Automation Science and Engineering* 2006; **3**(4): 360–371.
3. Alavi B, Pahlavan K. Modeling of the TOA-based distance measurement error using UWB indoor radio measurements. *IEEE Communications Letters* 2006; **10**(4): 275–277.
4. Chong C-C, Watanabe F, Win MZ. Effect of bandwidth on UWB ranging error. In *Proceedings of IEEE WCNC* 2007; 1561–1566.
5. Savvides A, Han C-C, Strivastava MB. Dynamic fine-grained localization in ad-hoc networks of sensors. In *Proceedings of ACM MobiCom* 2001; 166–179.
6. Ji X, Zha H. Robust sensor localization algorithm in wireless ad-hoc sensor networks. In *Proceedings of ICCCN* 2003; 527–532.
7. Chen JC, Hudson RE, Yao K. Maximum-likelihood source localization and unknown sensor location estimation for wideband signals in the near-field. *IEEE Transactions on Signal Processing* 2002; **50**(8): 1843–1854.
8. Biswas P, Ye Y. Semidefinite programming for ad hoc wireless sensor network localization. In *Proceedings of IPSN* 2004; 46–54.
9. Chang C, Sahai A. Estimation bounds for localization. In *Proceedings of IEEE SECON* 2004; 415–424.
10. Savvides A, Garber WL, Moses RL, Srivastava MB. An analysis of error inducing parameters in multihop sensor node localization. *IEEE Transactions on Mobile Computing* 2005; **4**(6): 567–577.
11. Urkowitz H. *Signal Theory and Random Processes*. Artech House: Dedham, MA, 1983.
12. Chang C. Localization and Object-Tracking in an Ultrawideband Sensor Network. *Master's Thesis*, EECS Department, University of California at Berkeley.
13. Drineas P, Javed A, Magdon-Ismail M, Pandurangan G, Virrankoski R, Savvides A. Distance matrix reconstruction from incomplete distance information for sensor network localization. In *Proceedings of IEEE SECON* 2006; 536–544.
14. Nocedal J, Wright SJ. *Numerical Optimization*. Springer: New York, 1999.
15. Wu S, Zhang Q, Fan R, Zhang N. Match-filtering based TOA estimation for IR-UWB ranging systems. *International Wireless Communications and Mobile Computing Conference* 2008 (submitted for publication).
16. Trosset MW. Extensions of classical multidimensional scaling via variable reduction. *Computational Statistics* 2002; **17**: 147–162.
17. Zhang X. *Matrix Analysis and Applications*. Tsinghua and Springer Publishing House: Beijing, 2004.
18. Blatt D, Hero AO, III. Energy-based sensor network source localization via projection onto convex sets. *IEEE Transactions on Signal Processing* 2006; **54**(9): 3614–3619.
19. Nan G-F, Li M-Q, Li J. Estimation of node localization with a real-coded genetic algorithm in WSNs. In *Proceedings of International Conference on Machine Learning and Cybernetics* 2007; 873–878.
20. Kannan AA, Mao G, Vucetic B. Simulated annealing based localization in wireless sensor network. In *Proceedings IEEE Conference on Local Computer Networks*, 2005.

Authors' Biographies

Rongfei Fan received his B.E. degree in 2007 in electrical engineering from Harbin Institute of Technology, China. He is currently a graduate student at the Department of Electrical and Computer Engineering, University of Alberta, Canada. His research interests include cognitive radio, ultra-wideband, and localization in wireless sensor networks.

Hai Jiang received his B.S. degree in 1995 and his M.S. degree in 1998, both in electronics engineering, from Peking University, China and his Ph.D. degree (with an Outstanding Achievement in Graduate Studies Award) in 2006 in electrical engineering from the University of Waterloo, Canada. He was a Postdoctoral Fellow at the Department of

DOI: 10.1002/wcm

Electrical Engineering, Princeton University from September 2006 to June 2007. Since July 2007, he has been an Assistant Professor at the Department of Electrical and Computer Engineering, University of Alberta, Canada. His research interests include radio resource management, cellular/WLAN interworking, and cross-layer design for wireless multimedia communications. He served as a Co-Chair for the General Symposium, International Wireless Communications and Mobile Computing Conference (IWCMC) 2007. He is an Associate Editor for the *IEEE Transactions on Vehicular Technology*.

Shaohua Wu received his B.E. degree in 2003 and his M.E. degree in 2005, both in electrical engineering, from Harbin Institute of Technology, China, where he is currently working toward his Ph.D. degree. His research interests include high-precision ranging in ultra-wideband radio technologies and localization in wireless sensor networks.

Naitong Zhang is currently a Professor at Harbin Institute of Technology, China. His research interests include mobile communications, satellite communications, and broadband networks.

DOI: 10.1002/wcm